

# Dihydroisoxazole Analogs for Labeling and Visualization of Catalytically Active Transglutaminase 2

Laila Dafik<sup>1</sup> and Chaitan Khosla<sup>1,2,\*</sup>

<sup>1</sup>Departments of Chemistry and Chemical Engineering

<sup>2</sup>Department of Biochemistry

Stanford University, Stanford, CA 94305, USA

\*Correspondence: [khosla@stanford.edu](mailto:khosla@stanford.edu)

DOI 10.1016/j.chembiol.2010.11.004

## SUMMARY

We report the synthesis and preliminary characterization of “clickable” inhibitors of human transglutaminase 2 (TG2). These inhibitors possess the 3-halo-4,5-dihydroisoxazole warhead along with bioorthogonal groups such as azide or alkyne moieties that enable subsequent covalent modification with fluorophores. Their mechanism for inhibition of TG2 is based on halide displacement, resulting in the formation of a stable imino thioether. Inhibition assays against recombinant human TG2 revealed that some of the clickable inhibitors prepared in this study have comparable specificity as benchmark dihydroisoxazole inhibitors reported earlier. At low micromolar concentrations they completely inhibited transiently activated TG2 in a WI-38 fibroblast scratch assay and could subsequently be used to visualize the active enzyme *in situ*. The potential use of these inhibitors to probe the role of TG2 in celiac sprue as well as other diseases is discussed.

## INTRODUCTION

Mammalian transglutaminases play important roles in many biological processes such as blood clotting, wound healing, extracellular matrix formation, and cell adhesion and motility (Akimov and Belkin, 2001; Fesus et al., 1987; Iismaa et al., 2009; Lorand, 2007; Lorand and Graham, 2003; Piacentini et al., 1991; Zemskov et al., 2006). Transglutaminase 2 (TG2), a ubiquitous member of this enzyme family, is found in intracellular as well as extracellular environments of many organs. In the presence of calcium and the absence of GTP or GDP, TG2 crosslinks selected  $\gamma$ -glutamyl and  $\epsilon$ -lysine residues on proteins, leading to the formation of proteolytically resistant covalent bonds. This catalytically active form of TG2 exists in an extended (“open”) conformation (Pinkas et al., 2007). In contrast, in the absence of calcium and the presence of GTP or GDP, TG2 assumes an inactive (“closed”) form (Liu et al., 2002) and functions as a G protein in the phospholipase C signal transduction cascade of the  $\alpha$ -adrenergic receptor (Nakaoka

et al., 1994; Singh et al., 1995). TG2 activity is also subject to regulation by local redox conditions (Stamnaes et al., 2010). Under oxidizing conditions, the formation of an intramolecular disulfide bond inactivates the enzyme; activity is reversibly restored under reducing conditions. Given the ubiquitous nature of TG2 and its ability to form covalent “scars,” its catalytic activity must be tightly regulated in mammals. However, the physiological signals that interconvert these active and inactive forms of the enzyme remain largely unknown. For example, whereas the majority of extracellular TG2 in the mouse small intestine is inactive, it can be rapidly activated at the villus tips by administration of poly(I:C), a ligand of the TLR-3 innate immune receptor (Siegel et al., 2008). Therefore, chemical probes of *in vivo* TG2 biology should be of considerable use in resolving some of these fundamental mysteries associated with allosteric TG2 regulation.

From a translational standpoint, TG2 is implicated in the pathogenesis of a number of unrelated disorders, including neurological diseases such as Huntington’s, Alzheimer’s, and Parkinson’s disease, certain types of cancers and renal diseases, and celiac sprue (Ruan and Johnson, 2007; Shweke et al., 2008; Verma and Mehta, 2007). For example, in celiac sprue, peptides derived from dietary gluten are deamidated by TG2 to enhance their affinity toward the disease-associated class II major histocompatibility complexes, which in turn activates inflammatory Th1 cells (Sollid and Lundin, 2009). Therefore, TG2 may be a suitable target for celiac sprue therapy. However, absent knowledge of the location, timing, and mechanism of TG2 activation in the celiac small intestine, this hypothesis cannot be rationally tested. Again, chemical probes could provide answers to these questions. Last, but not least, small molecule TG2 inhibitors could also serve as drug leads and eventually as drug candidates for one or more of the above diseases (Siegel and Khosla, 2007).

Many classes of irreversible, active site inhibitors of human TG2 have been reported thus far (Case et al., 2005; Choi et al., 2005; Freund et al., 1994; Halim et al., 2007; Hausch et al., 2003; Keillor, 2005; Pardin et al., 2006, 2008; Schaertl et al., 2010). One example is the 3-bromo-4,5-dihydroisoxazoles (DHIs) family of compounds (Castelhamo et al., 1988; Choi et al., 2005; Watts et al., 2006). Guided by the excellent tolerance of these molecules in acute and chronic administration studies in rodents (Choi et al., 2005; Yuan et al., 2007), here, we have used the DHI scaffold to develop a class of covalent TG2 probes

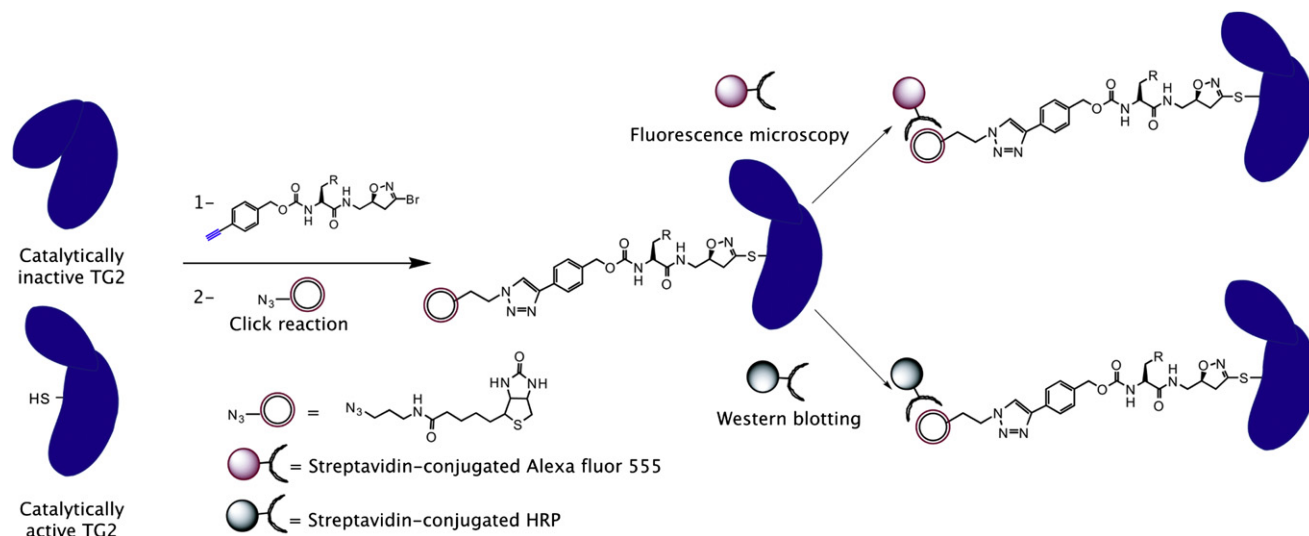


**Figure 1. Labeling and Visualization of Catalytically Active (but Not Catalytically Inactive) TG2 with Alkynyl-DHI Inhibitors**

Similar labeling strategy can be employed using azido-DHI inhibitors.

that bind to active but not inactive TG2 and can, therefore, be used to visualize the enzyme via a selective (bioorthogonal) chemical reaction (Figure 1). Analogous strategies have been used to modify cell surface glycans and proteins (Chin et al., 2002; Deiters and Schultz, 2005; Wang and Schultz, 2004), to profile protein glycosylation (Agard and Bertozzi, 2009), and for the detection of lipid-modified proteins (Hang et al., 2007). Recently, bioorthogonal chemical reporters have also been used in living animals as noninvasive imaging tools (Laughlin et al., 2008; Laughlin and Bertozzi, 2009; Prescher and Bertozzi, 2005).

## RESULTS

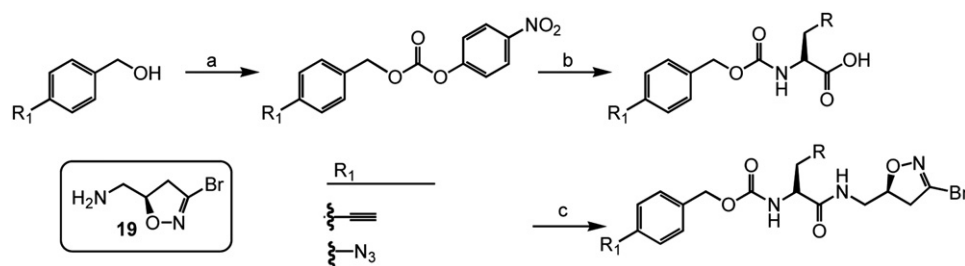
### Design and Synthesis of Azido- and Alkynyl-DHI Inhibitors

In this study we describe the synthesis and properties of DHI inhibitors of human TG2 that are conjugated to alkyne or azide functional groups. We incorporated alkyne and azide groups because of their bioorthogonality (Sletten and Bertozzi, 2009). Figure 2 describes the structure and synthesis of a representative

DHI inhibitor. Both azide and alkyne groups were introduced as substitutions on the carbobenzyloxy (Cbz) moiety because previous studies had highlighted the advantage of an aromatic group at this position (Watts et al., 2006). To identify a clickable inhibitor with optimal activity, we also varied the amino acid moiety of our DHI inhibitors using side chains that had previously been found to be beneficial. The compounds synthesized and evaluated in this study are summarized in Table 1; all of them were made in good yield and purity (see Supplemental Experimental Procedures and Figure S1 available online). Four previously synthesized DHI inhibitors, **13–16**, were chosen as reference compounds in this study; their TG2 inhibitory activities vary over an 8-fold range (Table 1).

### Inhibition of Recombinant Human TG2 by Azido- and Alkynyl-DHI Inhibitors

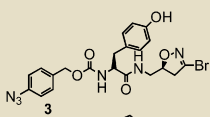
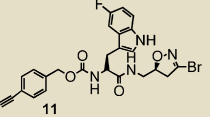
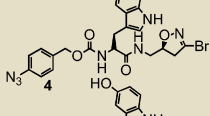
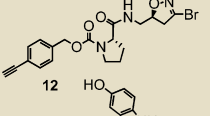
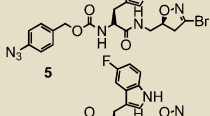
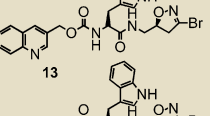
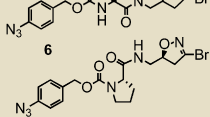
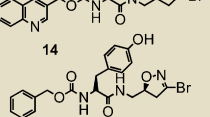
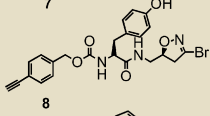
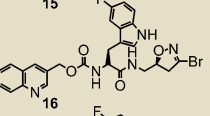
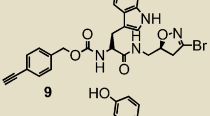
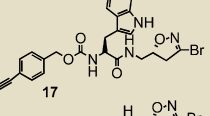
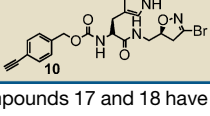
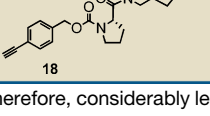
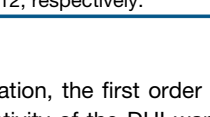
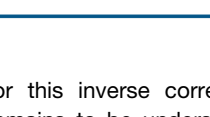
The potencies of alkynyl- and azido-DHI inhibitors **1–12** were evaluated in a kinetic assay using recombinant human TG2. In this assay, TG2-catalyzed deamidation of the dipeptide substrate Cbz-Gln-Gly is monitored under steady-state conditions. Analogous to the parameters of the Michaelis-Menten



**Figure 2. General Synthesis of Azido- and Alkynyl-DHI Inhibitors**

See Figure S1.

**Table 1. TG2 Inhibitory Activity of Enantiopure Azido- and Alkynyl-DHI Compounds**

Cmpd	$K_i$ ( $\mu\text{M}$ )	$k_{inh}$ ( $\text{min}^{-1}$ )	$k_{inh}/K_i$ ( $\text{mM}^{-1}\text{min}^{-1}$ )	Cmpd	$K_i$ ( $\mu\text{M}$ )	$k_{inh}$ ( $\text{min}^{-1}$ )	$k_{inh}/K_i$ ( $\text{mM}^{-1}\text{min}^{-1}$ )
	280	1.63	5.8		7.0	0.13	19
	15	0.23	15		1.8	0.052	30
	100	0.82	8.0		41	0.51	12
	19	0.31	16		47	0.53	11
	9.2	0.12	13		22	0.13	6.1
	4.2	0.016	4.0		19	0.73	38
	13	0.15	11		51	0.21	4.2
	12	0.14	8.0		38	0.27	7.2

Compounds 17 and 18 have a stereochemically altered DHI moiety and are, therefore, considerably less potent than their diastereomeric analogs, 11 and 12, respectively.

equation, the first order rate constant  $k_{inh}$  is a measure of the reactivity of the DHI warhead with the active site sulfhydryl of TG2, whereas  $K_i$  estimates the reversible binding affinity of the inhibitor to the active site. The bimolecular rate constant  $k_{inh}/K_i$  can be thought of as the specificity constant of TG2 for the inhibitor.

As summarized in Table 1, inhibitors harboring tryptophan analogs are more potent than those with tyrosine as the amino acid residue. Among tryptophan analogs, the 5-fluorotryptophan analogs have the highest specificity constants. The relative trends are similar between the azido-DHI and alkynyl-DHI inhibitor series. The most active alkynyl- and azido-DHI inhibitors (**12** and **6**, respectively) have specificity constants that are within 1.3- and 2.3-fold, respectively, of the most potent DHI inhibitor **16** identified to date. Together, these results encouraged us to evaluate some of these compounds in a cell culture assay for activated TG2.

It is noteworthy that the azido-DHI inhibitors prepared in this study have moderately higher TG2 specificity ( $k_{inh}/K_i$ ) than their alkynyl-DHI counterparts (Table 1). However, this benefit is primarily derived from higher reactivity toward the active site cysteine residue of TG2; the reversible binding affinity ( $K_i$ ) of the alkynyl-DHI inhibitors is actually higher. Although the reason

for this inverse correlation between affinity and specificity remains to be understood, in subsequent studies we placed greater emphasis on biological evaluations of the most promising alkynyl-DHI inhibitors.

#### Inhibition of TG2 in a Tissue Culture Wounding Model

To evaluate the activity of the clickable TG2 inhibitors identified above in a representative biological assay, we used a tissue culture wounding model. TG2 plays a role in wound healing in mammals by crosslinking extracellular matrix proteins after a wound has been inflicted. Recently, we demonstrated that, when a confluent monolayer of WI-38 fibroblast cells is scratched, TG2 is rapidly and transiently activated in the zone surrounding the "wound" (Siegel et al., 2008). This activated TG2 enzyme can be visualized using 5-biotinyl pentylamine (5BP), which presumably crosslinks onto glutamine side chains of fibronectin and other proteins along the scratch border that are recognized as TG2 substrates (Figure 3). Here, we have exploited this assay to compare the relative activities of TG2 inhibitors in a biological system.

To quantify inhibitor potency, selected inhibitors were added to scratched WI-38 cultures at incremental 2-fold dilutions. The lowest inhibitor concentration at which complete inhibition of

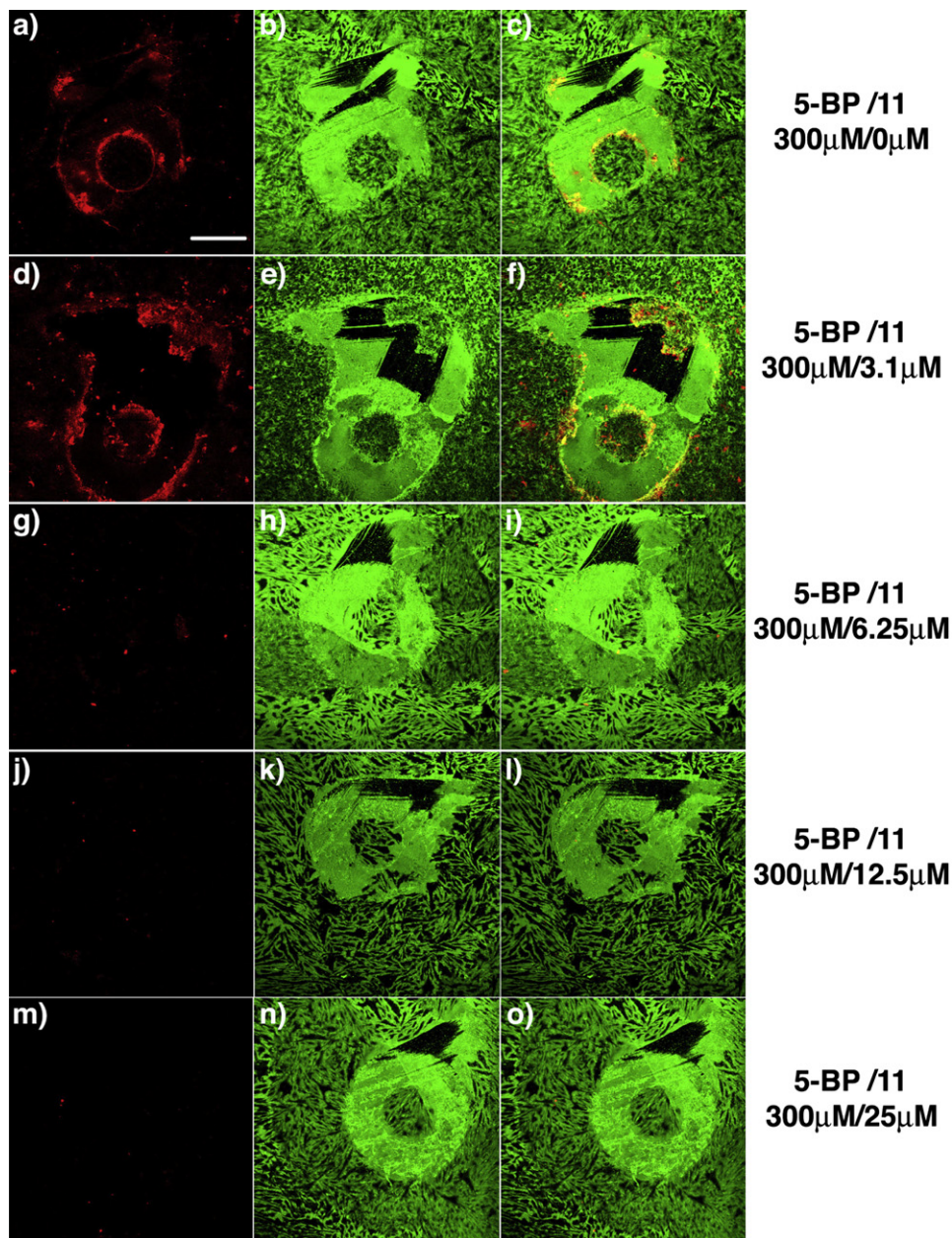


**Figure 3. Titration of **11** against Active TG2 in a Fibroblast Scratch Assay**

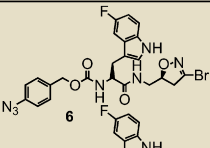
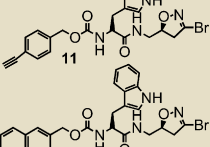
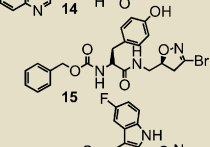
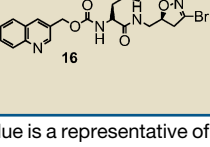
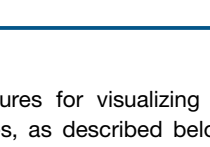
TG2 activity was visualized in situ after scratching a confluent WI-38 monolayer with a small pipette tip. Significant TG2 activity was detected around the wound in the presence of 300  $\mu\text{M}$  5BP and vehicle (DMSO) (A–C). Clear inhibition of active TG2 was observed in the presence of 6.25  $\mu\text{M}$  **11** (G–I), and complete inhibition was observed at or above 12.5  $\mu\text{M}$  **11** (J–O). In this assay, active TG2 was detected by exposing fixed cultures to streptavidin Alexa Fluor 555 (A, D, G, J, and M). The scratch geometry is conveniently visualized by co-staining with polyclonal anti-fibronectin antibody, followed by a secondary antibody conjugated Alexa Fluor 488 (B, E, H, K, and N). Overlays of the left and middle images are in the right column (C, F, I, L, and O). Scale bar represents 200  $\mu\text{m}$  and applies to all panels.

transiently activated TG2 was observed was recorded as the minimum inhibitory concentration (MIC) of that inhibitor. For example the effect of increasing concentrations of **11** on the extent of 5BP crosslinking around WI-38 scratches is shown in Figure 3; from these data, its MIC was estimated to lie between 6.25 and 12.5  $\mu\text{M}$ . The MIC values of different inhibitors are compared in Table 2 (see also Figures S2 and S3). Whereas the most potent inhibitors (e.g., **6**, **11**, **14**, and **16**) completely

blocked TG2 activity around the wound at 3.1–6.25  $\mu\text{M}$ , the less potent inhibitor **15** ( $k_{inh}/K_i = 6.1 \text{ mM}^{-1} \text{ min}^{-1}$ ) only showed partial inhibition at 25  $\mu\text{M}$ .

The above cell culture measurements verified that the biological potencies of the most active azido-DHI inhibitor (**6**) and the most active alkynyl-DHI inhibitors (**11** and **12**) were comparable to the benchmark DHI inhibitor of human TG2 (**16**) identified to date (Watts et al., 2006). This in turn encouraged us to develop

**Table 2. Titration of DHI Inhibitors against TG2 in a Fibroblast Wound Model**

Cmpd	MIC( $\mu$ M)
	[6.25-12.5]
	[6.25-12.5]
	[6.25-12.5]
	[50-75]
	[3.1-6.25]

Each value is a representative of three or more scratches. See [Figures S2 and S3](#).

procedures for visualizing inhibitor-bound TG2 in biological samples, as described below. Future improvements to these compounds will focus on improving their water solubility and rendering them resistant to chymotrypsin-catalyzed hydrolysis. Both properties would be necessary for chronic oral administration in animal studies directed at elucidating TG2 regulatory mechanisms in the small intestine and can be achieved by incorporating alternative amino acid residues or isosteres in place of 5-fluorotryptophan in compounds **6** and **11**.

### Labeling and Visualization of Catalytically Active TG2

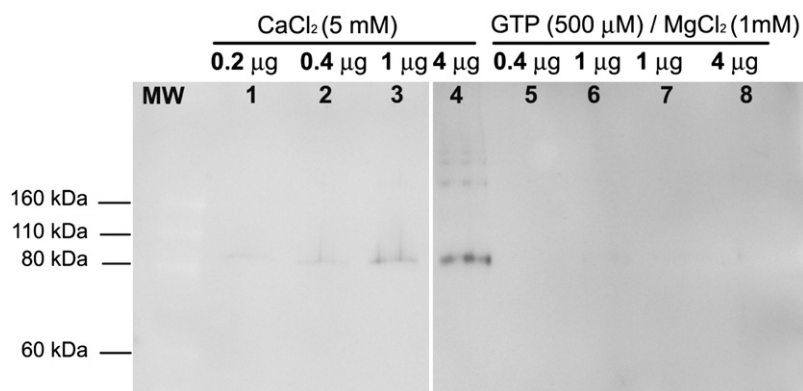
In principle the alkyne and azide groups incorporated into DHI inhibitors can be used as handles to selectively visualize the location of TG2 protein that is transiently activated in a biological sample. To test this hypothesis, alkynyl-inhibited TG2 was chemoselectively ligated to an azide-tagged biotin or fluorophore mole-

cule via a Cu<sup>1</sup>-catalyzed alkyne-azide [3+2] cycloaddition reaction ([Figure 1](#)). Initial experiments were performed with recombinant TG2 protein activated with Ca<sup>2+</sup> or inhibited with GTP. The proteins were resolved by gel electrophoresis and visualized by western blotting using neutravidin-linked horseradish peroxidase. Catalytically active TG2 treated with **12** can be efficiently conjugated with a suitable azide partner molecule and subsequently visualized in a dose-dependent manner ([Figure 4](#), lanes 1–4). The limit of detection of active TG2 by this western blotting method was below 1  $\mu$ g. GTP-bound, catalytically inactive TG2 was not labeled and, therefore, not visualized ([Figure 4](#), lanes 5–8).

To investigate the utility of this method for visualizing catalytically active TG2 in biological systems, we performed fluorescence microscopy on scratched WI-38 fibroblast cultures that had been incubated with two representative alkynyl-DHI inhibitors, **11** and **12**. In both cases, cells were extensively washed to remove excess inhibitor, fixed with paraformaldehyde (PFA), permeabilized with 0.1% Triton X-100, washed again, and subjected to the [3+2] cycloaddition reaction with biotin azide TG2 (active + inactive). The biotin conjugate was visualized by exposing fixed cultures to streptavidin conjugated with Alexa Fluor 555. The scratch was visualized with rabbit anti-fibronectin antibody, followed by exposure to an Alexa Fluor 488-conjugated goat anti-rabbit IgG secondary antibody.

Analogous to experiments with 5BP (see, for example, [Figure 3](#)), a strong red fluorescence signal was observed around the scratch in samples treated with inhibitors and reacted with biotin azide ([Figure 5](#); [Figure S4](#)), corresponding to catalytically active TG2. As negative controls, DMSO vehicle and two substantially weaker inhibitors, **17** and **18** ([Table 1](#)), were evaluated. These compounds, which are diastereomeric analogs of **11** and **12**, respectively, were used because earlier work had shown that TG2 specificity was strongly dependent upon the stereochemistry of the chiral center in the dihydroisoxazole ring. Scratches treated with **17** and **18** resulted in no red fluorescence around the scratch ([Figure 5](#); [Figure S4](#)).

Two other observations were made during the course of these studies with WI-38 fibroblasts. First, the signal-to-noise was significantly superior in scratches reacted with biotin azide as compared to rhodamine azide ([Figure S5](#)). The reason for this difference was not investigated. Second, 5BP yields a distinctly different labeling pattern around the fibroblast scratch than the

**Figure 4. Visualization of Recombinant TG2 with Alkynyl-DHI Inhibitor 12**

Recombinant TG2 was inhibited with **12** in the presence of CaCl<sub>2</sub> (5 mM) or GTP (500  $\mu$ M) and MgCl<sub>2</sub> (1 mM). The resulting mixture was reacted with biotin-azide, resolved by SDS-PAGE, and detected by western blotting with neutravidin-HRP. Lane 1 shows TG2 (0.2  $\mu$ g) + Ca<sup>2+</sup> + **12**; lane 2, TG2 (0.4  $\mu$ g) + Ca<sup>2+</sup> + **12**; lane 3, TG2 (1  $\mu$ g) + Ca<sup>2+</sup> + **12**; lane 4, TG2 (4  $\mu$ g) + Ca<sup>2+</sup> + **12**; lane 5, TG2 (0.4  $\mu$ g) + GTP/MgCl<sub>2</sub> + **12**; lane 6, TG2 (1  $\mu$ g) + GTP/MgCl<sub>2</sub> + **12**; lane 7, TG2 (1  $\mu$ g) + GTP/MgCl<sub>2</sub> + **12**; and lane 8, TG2 (4  $\mu$ g) + GTP/MgCl<sub>2</sub> + **12**.

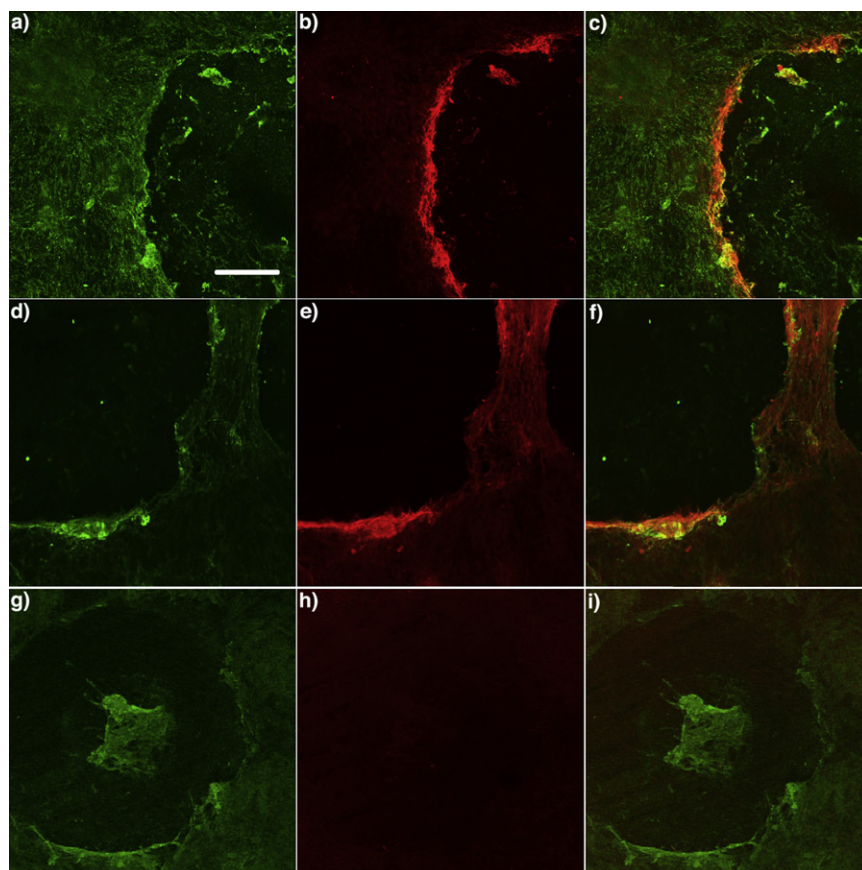


**Figure 5. Visualization of Catalytically Active TG2 in a Scratched WI-38 Fibroblast Culture**

TG2 activity was visualized after scratching confluent WI-38 monolayers in the presence of 50  $\mu$ M **11** (A–F) or **17** (G–I) for 1 hr. Cells were then fixed, permeabilized, reacted with biotin azide followed by streptavidin-Alexa Fluor 555 conjugates (red), and imaged by epifluorescence microscopy through a 10 $\times$  objective.

(A, D, and G) Rabbit anti-fibronectin antibody, followed by a secondary antibody labeled with Alexa Fluor 488, was used to visualize fibronectin on the WI-38 monolayers.

(B, E, and H) Catalytically active TG2 was visualized by coupling the alkynyl-DHI inhibitor to biotin azide.

(C, F, and I) Overlays of the left and middle image pairs are shown in the right column. Scale bar represents 200  $\mu$ m and applies to all panels.

See Figures S4 and S5.

clickable inhibitor. For example, whereas the overlap between red and green signals is excellent in Figure 3A, the two colors are proximal but clearly discernable in Figure 5E. Presumably, this is due to subtle differences in the distribution of catalytically active TG2 (i.e., the target of the clickable inhibitor) and its substrates (principally fibronectin, which is the target of 5BP) in the vicinity of the scratch.

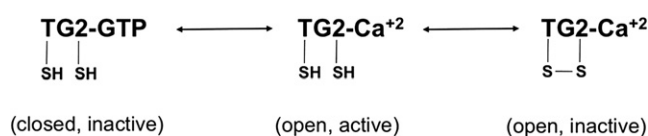
## DISCUSSION

Human TG2 catalyzes transamidation and deamidation reactions that are believed to contribute to a variety of physiological processes as well as to the pathogenesis of several diseases. Therefore, understanding the mechanisms responsible for spatiotemporal regulation of TG2 activity could have important implications for human biology and disease. However, because the protein is abundantly expressed in most organs and tissues, most mechanisms of interest are allosteric in nature, and conventional molecular biology approaches are not applicable. Consequently, new tools are needed to visualize rapid, tissue-specific transitions of TG2 from a catalytically inactive to an active state (or vice versa). Because TG2 is localized in multiple intracellular compartments as well as the extracellular environment, the ideal tools should also be able to resolve the subcellular location of the target protein. Here, we have described a new class of small molecule reagents that are well suited

for such a task. As shown, our clickable TG2 inhibitors can visualize the active enzyme in a manner that is only limited by the resolution of optical microscopy. Specifically, we have shown that compounds **11** and **12** can be used to visualize the burst of TG2 catalytic activity that rapidly appears at the scratch boundary of a WI-38 fibroblast cell culture system. Although the fibroblast scratch assay mimics a pathological rather than a physiological state, its utility for interrogating the allosteric transition of TG2 from an inactive to an active state has been established (Nicholas et al., 2003; Siegel et al., 2008). Our method has two principal advantages over previous studies that visualized transiently activated TG2 around scratched cells using amine substrates such as 5BP. First, whereas the use of amines only enables detection of TG2 substrates (principally fibronectin) that have undergone modification by catalytically active enzyme, our new method enables visualization of the activated enzyme itself. As illustrated by the differences between the labeling patterns around scratches in Figures 3 and 5, these differences may prove significant in further investigations of TG2 biology, especially in situations where subcellular resolution of the active enzyme is desired. Second, because the specificity of transglutaminases for their electrophilic (glutamine-bearing) substrates is considerably higher than for nucleophilic (amine-bearing) substrates, the development of isozyme-specific clickable DHI inhibitors should be feasible.

Pending verification of their *in vivo* stability, several important biological and medical problems could be addressed with clickable DHI inhibitors such as **11** and **12**. In metastatic cancers, TG2 is believed to play a crucial role in cell migration and has been shown to localize primarily at the leading edge of migrating cells (Antonyak et al., 2009). However, the relative importance of its catalytic versus signaling activity is unclear. For example the catalytically inactive C277S mutant of TG2 is

indistinguishable from the wild-type protein with respect to cell motility (Balklava et al., 2002). Visualizing the precise location(s) of catalytically active TG2 over the course of a nascent and metastasizing tumor could shed important light on the role of protein crosslinking in cancer. In celiac sprue the pathogenic role of catalytic TG2 is well established; however, the precise location at which catalytically active TG2 encounters immunotoxic gluten peptides remains a topic of controversy. Again, small molecule probes that can highlight the distribution of active enzyme in normal versus inflamed intestinal mucosa could be invaluable. More fundamentally, biochemical and structural biological investigations have demonstrated that TG2 undergoes allosteric changes between at least three distinct conformational states, as summarized in the scheme below:



Tools that can distinguish between the  $\text{Ca}^{+2}$ -bound active state versus the GTP-bound or disulfide-bonded inactive states could greatly facilitate a deeper understanding of the dynamics of this multifunctional protein in biological systems.

In conclusion, we also note that our lead clickable inhibitors reported here could be further improved with respect to several characteristics. First, they have relatively low solubility in aqueous buffers. The efficiency of labeling TG2-bound inhibitors via [3+2] cycloaddition could also be improved by varying the spacer length between the alkyne and the benzyl groups. Last, but not least, the reactivity of these inhibitors with other mammalian transglutaminases could be further engineered in order to develop probes with orthogonal specificity for individual isozymes of this protein family.

## SIGNIFICANCE

**We have developed nonradioactive chemical probes for detecting and imaging catalytically active transglutaminase 2 (TG2) in mammalian cells and tissues. A series of electrophilic dihydroisoxazole compounds have been engineered with alkyne and azide groups that can be further modified by "click chemistry" ( $\text{Cu}^1$ -catalyzed alkynyl-azide [3+2] cycloaddition). These compounds have high specificity for the TG2 active site and undergo an irreversible reaction with the catalytically active cysteine residue. The biological utility of these mechanism-based irreversible inhibitors is demonstrated by their ability to visualize transiently activated TG2 in a fibroblast scratch assay. These probes should be broadly useful in elucidating mechanisms responsible for allosteric regulation of this multifunctional protein in cell biology, mammalian development, as well as a variety of human diseases.**

## EXPERIMENTAL PROCEDURES

### Cell Culture and Antibodies

WI-38 fibroblasts were grown in minimum essential media (GIBCO; 11095) containing L-glutamine, Earle's salts, nonessential amino acids (GIBCO; 11140), sodium pyruvate (GIBCO; 11360), 10% fetal bovine serum (FBS

(Atlanta Biologicals), and 100 U/ml penicillin + 100  $\mu\text{g}/\text{ml}$  streptomycin (GIBCO; 15140). Cells were typically grown to 80%–90% confluency before treating with trypsin-EDTA (GIBCO; 15400) and splitting. All cells were grown in a humidified incubator at 37°C, 5%  $\text{CO}_2$ . The antibodies used were anti-fibronectin antibody produced in Rabbit (Sigma-Aldrich; F3648), Alexa Fluor 488 goat anti-rabbit IgG (H-L) antibody (Invitrogen; A-11008), and Alexa Fluor 555-labeled streptavidin (Invitrogen; S-21381).

### Synthesis of Alkynyl- and Azido-DHI Inhibitors

Compounds **3–18** were synthesized as previously reported (Watts et al., 2006). Briefly, 4-ethynylbenzyl alcohol was reacted with *p*-nitrophenyl chloroformate in methylene chloride and *N*-methylmorpholine to give a carbonate of 4-ethynyl benzyl and *p*-nitrophenol after purification by flash chromatography. The carbonate was reacted with the methyl ester of the amino acid in DMF and *N*-methylmorpholine to give 4-ethynyl benzyl carbamate protected amino acid methyl ester. Methyl ester hydrolysis, followed by EDCI coupling of resulting acid to the (*S*)-isomer of the halo-dihydroisoxazole, gave the indicated compound as a final product after flash chromatography purification. The azido-DHI compounds were synthesized in similar fashion.

### TG2 Inhibition Assays

Recombinant human TG2 was expressed in *E. coli* and purified to >90% homogeneity as described previously (Choi et al., 2005). The potency of individual DHI inhibitors was assayed in a reaction mixture containing 200 mM MOPS (pH 7.2), 5 mM  $\text{CaCl}_2$ , 1 mM EDTA, 10 mM  $\alpha$ -ketoglutarate, 18 U/ml glutamate dehydrogenase, 0.4 mM NADH, 3.3% (v/v) DMSO, 0.5  $\mu\text{M}$  TG2, and 10, 20, and 30 mM Cbz-Gln-Gly ( $K_M = 6.28$  mM,  $k_{\text{cat}} = 37$   $\text{min}^{-1}$ ). The concentration of each inhibitor was varied from 0.001 to 0.3 mM. The reaction was initiated by adding TG2, and the consumption of NADH was monitored by UV spectroscopy (340 nm,  $\epsilon = 6220$   $\text{cm}^{-1} \text{M}^{-1}$ ). Kinetic parameters were obtained by plotting the reaction progress curves against theoretical equations for irreversible enzyme inhibition.

### Labeling and Visualization of TG2 with Clickable Inhibitors

TG2 protein was subjected to the probe labeling in 50  $\mu\text{l}$  volume reaction containing a final concentration of 2 mM of **12**, and 5 mM  $\text{CaCl}_2$  or 500 mM GTP/1 mM  $\text{MgCl}_2$  in 100 mM Tris HCl (pH 7.2) for 1 hr at RT. Then, 2 mM of biotin azide was added, 1 mM tris(2-carboxyethyl)phosphine hydrochloride (TCEP; Sigma-Aldrich) dissolved in water, 0.2 mM tris[(1-benzyl-1*H*-1,2,3-triazole-4-yl)methyl]amine (TBTA; Sigma-Aldrich) dissolved in DMSO/*tert*-butanol (20%/80%), and 1 mM  $\text{CuSO}_4$  in PBS. The reaction was quenched with 2 $\times$  loading buffer. Samples were resolved by SDS-PAGE using 4%–20% Tris-glycine gels and transferred onto a nitrocellulose membrane. The membrane was blocked with PBS, 0.1% Tween 20 (PBST), and 5% nonfat dried milk for 1 hr at RT. The membrane was washed three times with PBST (5 min each) and incubated with neutravidin-horseradish peroxidase (Invitrogen; 1:200 in 5% nonfat dried milk) for 1 hr at RT. The membrane was washed again with PBST three times (10 min each) and developed according to manufacturer's recommendation (Amersham Biosciences).

### Detection of TG2 Activity in Fibroblast Scratch Assays Using 5BP

WI-38 fibroblasts were plated in an 8-well chamber glass slide at  $2 \times 10^5$  cells/well and grown for 3 days with medium change every 2 days. Small scratches were made in the monolayer with 0.1–10  $\mu\text{l}$  pipette tip, and the cells were incubated with 5BP for 1 hr at 37°C, 5%  $\text{CO}_2$ . To capture the highest TG2 activity around the wound, we performed titration assays using 50, 100, 150, and 300  $\mu\text{M}$  5BP; the best results were obtained at 300  $\mu\text{M}$  5BP. To quantify TG2 inhibition in cultured cells, inhibitors **3–18** were added at the indicated concentrations to the culture media for 10–15 min. An equal amount of vehicle (DMSO) was added to the media of control cells at 37°C. Then, 5BP was added at a final concentration 300  $\mu\text{M}$  and incubated for an additional 1 hr at 37°C, 5%  $\text{CO}_2$ . The cells were washed three times with PBS and fixed with –20°C methanol for 10 min. Fixed cells were washed again with PBS twice for 5 min, blocked with 1% BSA in PBS for 15 min at room temperature, and washed twice more with PBS. Anti-fibronectin antibody produced in Rabbit (F3648; Sigma-Aldrich) was diluted 1:500 in blocking buffer and incubated for 1 hr at RT. Cells were washed three times with PBS and incubated with Alexa Fluor 488 goat anti-rabbit IgG (H<sup>+</sup>L) (A-11034; Invitrogen) and Alexa Fluor

555-streptavidin conjugate in blocking buffer for 1 hr at RT. After three further washes with PBS, 300  $\mu$ l PBS was added onto each sample before visualization via fluorescence microscopy. Note that Factor XIII, another ubiquitous member of the transglutaminase family, is not expressed in WI-38 fibroblasts (data not shown).

#### Detection of TG2 Activity in Fibroblast Scratch Assays Using Clickable Inhibitors

Following WI-38 fibroblast cell growth and scratching as above, compounds **11** and **12** were added to living cells for 10–15 min at 50  $\mu$ M final concentration at 37°C, 5% CO<sub>2</sub>. Control cells were incubated with 300  $\mu$ M 5BP and vehicle (DMSO). Cells were washed three times with PBS to remove excess compounds and fixed with 4% PFA for 10 min at RT. Cells were then permeabilized with PBS/0.1% Triton X-100 for 1–2 min at RT, washed extensively with PBS, and subjected to the [3+2] cycloaddition reaction at RT for 1 hr in 175  $\mu$ l solution containing 1 mM biotin azide, 1 mM TCEP dissolved in water, and 1 mM CuSO<sub>4</sub> in PBS. The labeled samples were rinsed extensively with PBS and blocked in PBS/5% BSA for 45 min at RT. To visualize the fibronectin protein, samples were treated with rabbit anti-fibronectin for 1 hr at RT in PBS/5%BSA, then washed three times with PBS, and further stained with the goat anti-Rabbit Alexa Fluor 488-conjugated secondary antibody for 45 min in PBS/5% BSA at RT. After three further washes, 300  $\mu$ l of PBS was added onto the cells for visualization via microscopy. Fluorescent images were captured in an upright Zeiss microscope.

#### SUPPLEMENTAL INFORMATION

Supplemental Information includes Supplemental Experimental Procedures and five figures and can be found with this article online at [doi:10.1016/j.chembiol.2010.11.004](https://doi.org/10.1016/j.chembiol.2010.11.004).

#### ACKNOWLEDGMENTS

This work was supported by a grant from the NIH (R01 DK063158) to C.K. L.D. is a recipient of a postdoctoral fellowship from "Fonds de Recherche sur la Nature et les Technologies" (Canada).

Received: July 27, 2010

Revised: November 2, 2010

Accepted: November 2, 2010

Published: January 27, 2011

#### REFERENCES

- Agard, N.J., and Bertozzi, C.R. (2009). Chemical approaches to perturb, profile, and perceive glycans. *Acc. Chem. Res.* **42**, 788–797.
- Akimov, S.S., and Belkin, A.M. (2001). Cell surface tissue transglutaminase is involved in adhesion and migration of monocytic cells on fibronectin. *Blood* **98**, 1567–1576.
- Antonyak, M.A., Li, B., Regan, A.D., Feng, Q.Y., Dusaban, S.S., and Cerione, R.A. (2009). Tissue transglutaminase is an essential participant in the epidermal growth factor-stimulated signaling pathway leading to cancer cell migration and invasion. *J. Biol. Chem.* **284**, 17914–17925.
- Balklava, Z., Verderio, E., Collighan, R., Gross, S., Adams, J., and Griffin, M. (2002). Analysis of tissue transglutaminase function in the migration of Swiss 3T3 fibroblasts: the active-state conformation of the enzyme does not affect cell motility but is important for its secretion. *J. Biol. Chem.* **277**, 16567–16575.
- Case, A., Ni, J., Yeh, L.A., and Stein, R.L. (2005). Development of a mechanism-based assay for tissue transglutaminase—results of a high-throughput screen and discovery of inhibitors. *Anal. Biochem.* **338**, 237–244.
- Castelano, A.L., Billedeau, R., Pliura, D.H., Bonaventura, B.J., and Krantz, A. (1988). Synthesis, chemistry, and absolute-configuration of novel transglutaminase inhibitors containing a 3-halo-4,5-dihydroisoxazole. *Bioorg. Chem.* **16**, 335–340.
- Chin, J.W., Santoro, S.W., Martin, A.B., King, D.S., Wang, L., and Schultz, P.G. (2002). Addition of p-azido-L-phenylalanine to the genetic code of *Escherichia coli*. *J. Am. Chem. Soc.* **124**, 9026–9027.
- Choi, K., Siegel, M., Piper, J.L., Yuan, L., Cho, E., Strnad, P., Omary, B., Rich, K.M., and Khosla, C. (2005). Chemistry and biology of dihydroisoxazole derivatives: selective inhibitors of human transglutaminase 2. *Chem. Biol.* **12**, 469–475.
- Deiters, A., and Schultz, P.G. (2005). In vivo incorporation of an alkyne into proteins in *Escherichia coli*. *Bioorg. Med. Chem. Lett.* **15**, 1521–1524.
- Fesus, L., Thomazy, V., and Falus, A. (1987). Induction and activation of tissue transglutaminase during programmed cell death. *FEBS Lett.* **224**, 104–108.
- Freund, K.F., Doshi, K.P., Gaul, S.L., Claremon, D.A., Remy, D.C., Baldwin, J.J., Pitzenger, S.M., and Stern, A.M. (1994). Transglutaminase inhibition by 2-[(2-oxopropyl)thio]imidazolium derivatives: mechanism of factor XIIIa inactivation. *Biochemistry* **33**, 10109–10119.
- Halim, D., Caron, K., and Keillor, J.W. (2007). Synthesis and evaluation of peptidic maleimides as transglutaminase inhibitors. *Bioorg. Med. Chem. Lett.* **17**, 305–308.
- Hang, H.C., Geutjes, E.J., Grotenbreg, G., Pollington, A.M., Bijlmakers, M.J., and Ploegh, H.L. (2007). Chemical probes for the rapid detection of fatty-acylated proteins in mammalian cells. *J. Am. Chem. Soc.* **129**, 2744–2745.
- Hausch, F., Halttunen, T., Maki, M., and Khosla, C. (2003). Design, synthesis, and evaluation of gluten peptide analogs as selective inhibitors of human tissue transglutaminase. *Chem. Biol.* **10**, 225–231.
- lismaa, S.E., Mearns, B.M., Lorand, L., and Graham, R.M. (2009). Transglutaminases and disease: lessons from genetically engineered mouse models and inherited disorders. *Physiol. Rev.* **89**, 991–1023.
- Keillor, J.W. (2005). Tissue transglutaminase inhibition. *Chem. Biol.* **12**, 410–412.
- Laughlin, S.T., and Bertozzi, C.R. (2009). In vivo imaging of *Caenorhabditis elegans* glycans. *ACS Chem. Biol.* **4**, 1068–1072.
- Laughlin, S.T., Baskin, J.M., Amacher, S.L., and Bertozzi, C.R. (2008). In vivo imaging of membrane-associated glycans in developing zebrafish. *Science* **320**, 664–667.
- Liu, S., Cerione, R.A., and Clardy, J. (2002). Structural basis for the guanine nucleotide-binding activity of tissue transglutaminase and its regulation of transamidation activity. *Proc. Natl. Acad. Sci. USA* **99**, 2743–2747.
- Lorand, L. (2007). Crosslinks in blood: transglutaminase and beyond. *FASEB J.* **21**, 1627–1632.
- Lorand, L., and Graham, R.M. (2003). Transglutaminases: crosslinking enzymes with pleiotropic functions. *Nat. Rev. Mol. Cell Biol.* **4**, 140–156.
- Nakaoka, H., Perez, D.M., Baek, K.J., Das, T., Husain, A., Misono, K., Im, M.J., and Graham, R.M. (1994). Gh: a GTP-binding protein with transglutaminase activity and receptor signaling function. *Science* **264**, 1593–1596.
- Nicholas, B., Smethurst, P., Verderio, E., Jones, R., and Griffin, M. (2003). Cross-linking of cellular proteins by tissue transglutaminase during necrotic cell death: a mechanism for maintaining tissue integrity. *Biochem. J.* **371**, 413–422.
- Pardin, C., Gillet, S., and Keillor, J.W. (2006). Synthesis and evaluation of peptidic irreversible inhibitors of tissue transglutaminase. *Bioorg. Med. Chem.* **14**, 8379–8385.
- Pardin, C., Pelletier, J.N., Lubell, W.D., and Keillor, J.W. (2008). Cinnamoyl inhibitors of tissue transglutaminase. *J. Org. Chem.* **73**, 5766–5775.
- Piacentini, M., Autuori, F., Dini, L., Farrace, M.G., Ghibelli, L., Piredda, L., and Fesus, L. (1991). Tissue transglutaminase is specifically expressed in neonatal rat liver cells undergoing apoptosis upon epidermal growth factor-stimulation. *Cell Tissue Res.* **263**, 227–235.
- Pinkas, D.M., Strop, P., Brunger, A.T., and Khosla, C. (2007). Transglutaminase 2 undergoes a large conformational change upon activation. *PLoS Biol.* **5**, e327.
- Prescher, J.A., and Bertozzi, C.R. (2005). Chemistry in living systems. *Nat. Chem. Biol.* **1**, 13–21.

- Ruan, Q., and Johnson, G.V. (2007). Transglutaminase 2 in neurodegenerative disorders. *Front. Biosci.* *12*, 891–904.
- Schaertl, S., Prime, M., Wityak, J., Dominguez, C., Munoz-Sanjuan, I., Pacifici, R.E., Courtney, S., Scheel, A., and Macdonald, D. (2010). A profiling platform for the characterization of transglutaminase 2 (TG2) inhibitors. *J. Biomol. Screen.* *15*, 478–487.
- Shweke, N., Boulou, N., Jouanneau, C., Vandermeersch, S., Melino, G., Dussaule, J.C., Chatziantoniou, C., Ronco, P., and Boffa, J.J. (2008). Tissue transglutaminase contributes to interstitial renal fibrosis by favoring accumulation of fibrillar collagen through TGF-beta activation and cell infiltration. *Am. J. Pathol.* *173*, 631–642.
- Siegel, M., and Khosla, C. (2007). Transglutaminase 2 inhibitors and their therapeutic role in disease states. *Pharmacol. Ther.* *115*, 232–245.
- Siegel, M., Strnad, P., Watts, R.E., Choi, K.H., Jabri, B., Omary, M.B., and Khosla, C. (2008). Extracellular transglutaminase 2 is catalytically inactive, but is transiently activated upon tissue injury. *PLoS ONE* *3*, e1861.
- Singh, U.S., Erickson, J.W., and Cerione, R.A. (1995). Identification and biochemical characterization of an 80 kilodalton GTP-binding transglutaminase from rabbit liver nuclei. *Biochemistry* *34*, 15863–15871.
- Sletten, E.M., and Bertozzi, C.R. (2009). Bioorthogonal chemistry: fishing for selectivity in a sea of functionality. *Angew. Chem. Int. Ed. Engl.* *48*, 6974–6998.
- Sollid, L.M., and Lundin, K.E.A. (2009). Diagnosis and treatment of celiac disease. *Mucosal Immunol.* *2*, 3–7.
- Stamnaes, J., Pinkas, D.M., Fleckenstein, B., Khosla, C., and Sollid, L.M. (2010). Redox regulation of transglutaminase 2 activity. *J. Biol. Chem.* *285*, 25402–25409.
- Verma, A., and Mehta, K. (2007). Tissue transglutaminase-mediated chemoresistance in cancer cells. *Drug Resist. Updat.* *10*, 144–151.
- Wang, L., and Schultz, P.G. (2004). Expanding the genetic code. *Angew. Chem. Int. Ed. Engl.* *44*, 34–66.
- Watts, R.E., Siegel, M., and Khosla, C. (2006). Structure-activity relationship analysis of the selective inhibition of transglutaminase 2 by dihydroisoxazoles. *J. Med. Chem.* *49*, 7493–7501.
- Yuan, L., Siegel, M., Choi, K., Khosla, C., Miller, C.R., Jackson, E.N., Piwnicka-Worms, D., and Rich, K.M. (2007). Transglutaminase 2 inhibitor, KCC009, disrupts fibronectin assembly in the extracellular matrix and sensitizes orthotopic glioblastomas to chemotherapy. *Oncogene* *26*, 2563–2573.
- Zemskov, E.A., Janiak, A., Hang, J., Waghray, A., and Belkin, A.M. (2006). The role of tissue transglutaminase in cell-matrix interactions. *Front. Biosci.* *11*, 1057–1076.